Lateral templating of self-organized ripple morphologies during focused ion beam milling of Ge

Stefan Ichim and Michael J. Aziz
Division of Engineering and Applied Sciences, Harvard University, Cambridge, Massachusetts 02138

(Received 28 May 2004; accepted 22 February 2005; published 2 June 2005)

We report the use of the boundary between ion irradiated and unirradiated regions to template the lateral self-organization of nanoscale ripplelike morphological features that spontaneously evolve during uniform ion irradiation. Using uniform rastering of a 30 keV Ga^+ focused ion beam, up to eight periods of ripples have been templated to follow the boundary under the set of conditions explored. We report the dependence of the range of lateral templating on incident angle, ion dose, and boundary inclination with respect to the projected ion beam direction. We show that the ripple organization is influenced by a down-step as well as by an up-step in the surface morphology. © *2005 American Vacuum Society.* [DOI: 10.1116/1.1897711]

Because the future of nanotechnology ultimately rests on the controllable and cost-effective fabrication, integration, and mass production of nanoscale structures, various fabrication and assembly techniques are being investigated. Photolithography permits excellent throughput and morphology control but is approaching fundamental limitations to the further reduction of feature sizes. Single-particle manipulation techniques permit exquisite control but are challenged by throughput considerations. Self-organization processes are more readily adapted to high throughput but are challenged by limitations in control.

Solid surfaces sputter-eroded by uniform ion irradiation are known to undergo a morphological instability termed "sputter-rippling."[1] This phenomenon has also been observed under ion milling conditions with a focused ion beam (FIB), even in situations where the raster pattern is designed for uniform etching of a large area.[2–4] In many cases the morphological instability is considered a nuisance.[5] However, the observations that the ripple wavelength is a controllable function of the irradiation conditions[5,6] and that sublithographic feature sizes can be created have stimulated interest in the investigation of this phenomenon as a possible nanofabrication technique. Additionally, ion irradiation of Ge and of some III-V compounds has been shown to result in three-dimensional structures with feature sizes as small as 15 nm and very large aspect ratios.[3,4,7] Although fabrication with the FIB itself is not envisaged as a mass production technique, unfocused ion irradiation is already in mass production in CMOS processing, and it is anticipated that the rapid feedback possible with *in situ* real-space imaging in a FIB instrument will accelerate the understanding of the phenomena believed to be common to both focused and unfocused ion irradiation.

It has been observed occasionally that the sputter ripple pattern resulting from irradiation is influenced by the boundaries of the irradiated region.[3,4] In this work we explore this phenomenon for the case of 30 keV Ga^+ FIB irradiation of Ge(001) at room temperature. Irradiation was carried out using a FEI DualBeam DB235 FIB-Scanning Electron Microscope (SEM) in a vacuum of $\sim 1.4\times 10^{-6}$ mbar. The beam current was 100 pA and the spot size was nominally 20 nm. The beam was rastered across a predefined area of the sample surface, during which the beam would dwell at each discrete location for 1 μs and then move rapidly to an adjacent location. The direction of motion was normal to the projected ion beam direction except at the edges where the path "turned around." The separation between adjacent locations was set to nominally 50% overlap, which in this case meant a 10 nm center-to-center spacing in a plane normal to the ion beam direction. The current profile within the beam is believed to be roughly Gaussian. The morphology of the irradiated surface was observed using *in situ* SEM.

In Fig. 1 we show an example of the ripple structure resulting from typical conditions. A series of rectangular craters was created using exposures of 1–12 min, in 1 min increments, at an incident angle of 62° from normal. The projected ion beam direction is from left to right in the figure. The "upstream" ripples, i.e., those near the left edge of the crater, are more contiguous and better aligned to the boundary than the "downstream" ripples. The ripple wavelength starts at around 200 nm and coarsens slowly with increasing dose (reported throughout this paper as ions per cm^2 in a plane perpendicular to the ion beam). The length scale of the ripples is not only much larger than the spot size and dot pitch reported above, but is also much larger than the ion range (17 nm), longitudinal straggling (10 nm standard deviation), and transverse straggling (7 nm standard deviation) calculated by SRIM.[8]

In Fig. 2 we show the result of an experiment to isolate the effect of the boundaries of the rastered area from the effects of the projected ion beam direction and the scan direction. An irregular quadrilateral has been rastered such that none of the boundaries are normal to the projected ion beam direction. The raster path, however, is vertical in the figure. The first four ripples are extremely well aligned to the boundary, as indicated by the dashed lines. The alignment decays with distance so that only about 50% of the seventh ripple is aligned to the boundary. The tenth ripple and beyond appear completely uninfluenced by the boundary, the wave vector now being parallel to the projected ion beam

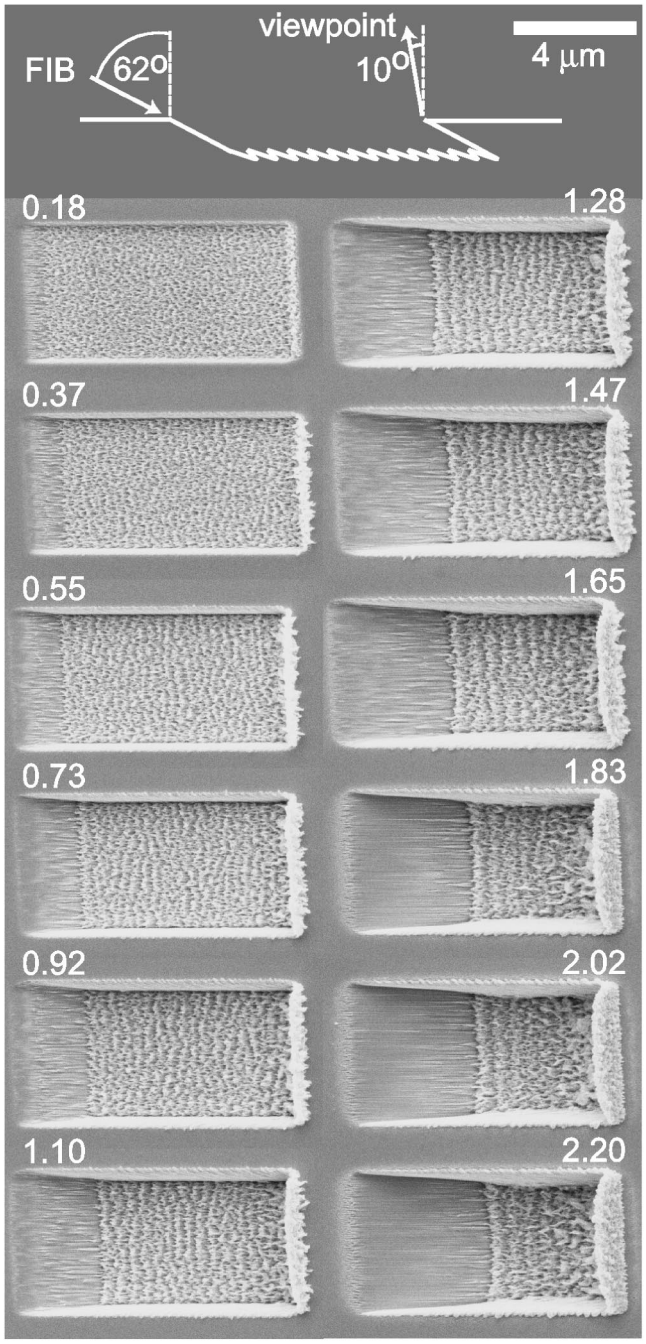

FIG. 1. Ripple alignment with boundary of FIB-milled rectangle. Plan-view SEM image of successive craters created using ion exposures of 1–12 min, in 1 min increments, from upper left through lower right. Dose in units of $10^{18}/\mathrm{cm}^2$ is indicated immediately above each micrograph. Side view illustrating milling and imaging geometry is shown at the top. The higher contiguity and better alignment of the "upstream" ripples, i.e., those near the left edge of the crater, compared to those downstream is most apparent in the images at the top of the right-hand column. Ripples farthest downstream are hidden by overhang in high-dose images; actual area of crater bottom is independent of dose. Crater depth in final frame is 1.5 μm. Beam current was 100 pA; beam diameter was 20 nm; center-to-center spacing was 10 nm.

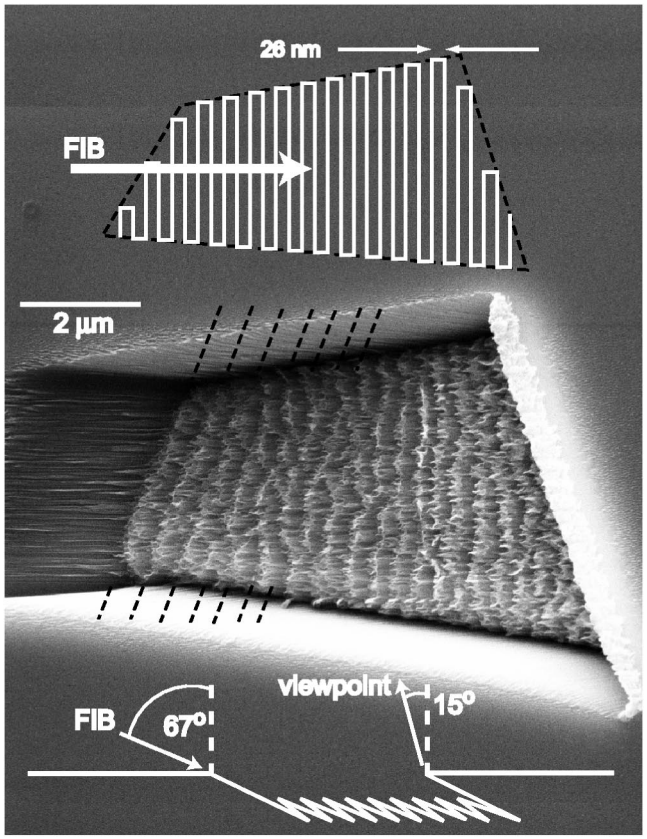

FIG. 2. Ripple alignment with boundary of FIB-milled irregular quadrilateral. SEM image taken at 15° from normal. Ion irradiation 67° from normal, projected ion beam direction shown by arrow; ion dose of $0.4\times10^{18}/\mathrm{cm}^2$. Schematic cross section shown at the bottom. Schematic of raster pattern in plan view is shown at the top. Raster path is the white line; left boundary of the raster pattern is inclined by 10°. Note that the actual line pitch of the raster is much smaller than drawn, 10 nm/cos(67°), or 26 nm. Ripple alignment with boundary near left edge decays over several periods until ripples align normal to the projected ion beam in the center of the milled region. Diagonal lines drawn along the ripples are guides to the eye.

direction. We identify the "number of aligned ripples" as seven in this case. We identify a ripple as "aligned" if it appears, by visual inspection of the micrographs, to run in a direction parallel to the boundary for a significant fraction (~50%) of the span of the crater. We estimate the uncertainty in the number of aligned ripples identified in this manner to be ±2 when values are in this range, and proportionately less for smaller values.

In Fig. 3 we show that the ripples can be aligned also by a "down step" as opposed to an "up step." Trenches with inclined boundaries were initially milled to an unspecified, large depth. A subsequent rectangular raster partially overlapping the trenches created ripples with alignment controlled by the inclination of the trench boundary.

The extent of alignment is a nonmonotonic function of ion dose. In Fig. 4 we plot the number of aligned ripples and the ripple wavelength vs. dose for a rectangular crater milled in the geometry of Fig. 1. A maximum in number of aligned ripples is observed near $1.4\times10^{18}/\mathrm{cm}^2$. The extent of lateral influence of the boundaries can reach 2 μm at this point. The breakdown of the ordering at larger doses appears to be the result of homogeneous coarsening and break-up of the ripples.

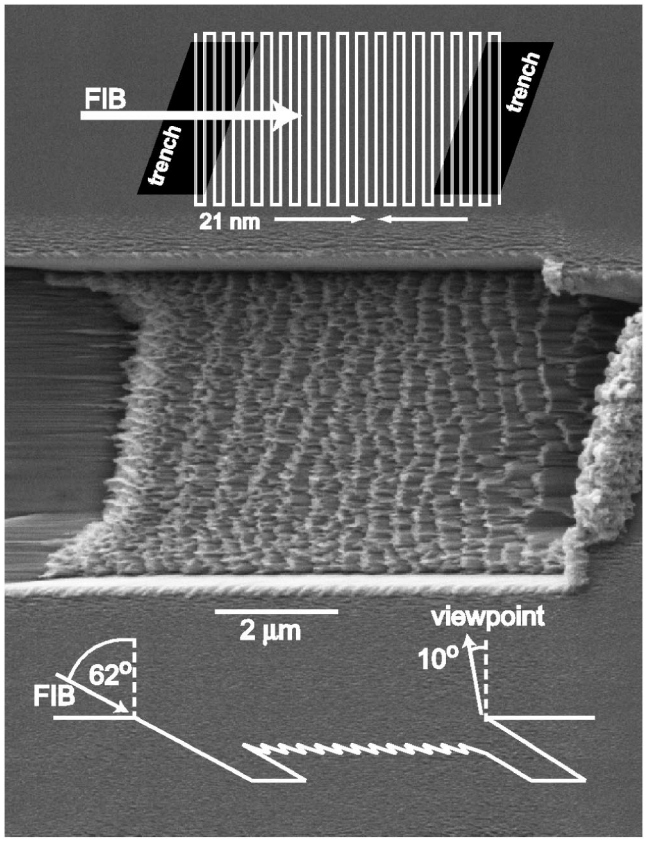

FIG. 3. Ripple alignment with trenches. SEM image taken at 10° from normal. Ion irradiation at 62° from normal, projected ion beam direction showed by arrow. Schematic cross section at bottom and plan view at top. Trenches with boundaries inclined by 62° from normal to projected ion beam direction were initially milled to create "down-steps" for templating of ripples. Rectangular raster partially overlapped trenches as shown. Raster path is white line. Ripple alignment with boundary near "upstream" edge decays over several periods.

Ripple alignment is sensitive to the angle of incidence of the FIB. In Fig. 5 we plot the number of aligned ripples vs incidence angle with respect to the surface normal. All irradiations were for 400 s, corresponding to a dose of $1.68 \times 10^{18}/\mathrm{cm}^2$. (As the angle increases from zero, the dose reckoned in a plane parallel to the wafer surface decreases from this value to $0.66 \times 10^{18}/\mathrm{cm}^2$ for 67°.) The alignment appears to be still increasing with angle at the most grazing incidence angle that we could attain with the existing sample holder. Still greater angles should be attainable using a refined geometry.

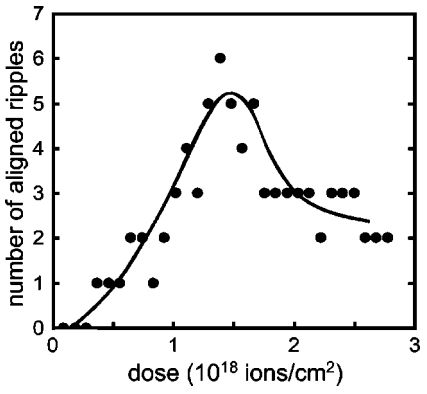

FIG. 4. Dose dependence of number of aligned ripples for the geometry of Fig. 1. Line is a guide to the eye.

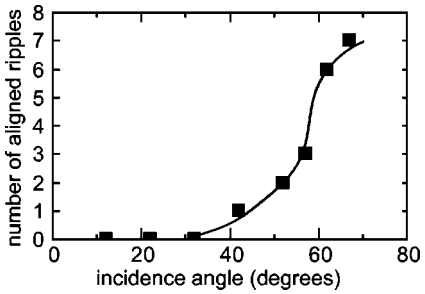

FIG. 5. Number of aligned ripples vs incidence angle with respect to surface normal. All irradiations were for $1.7 \times 10^{18}/\mathrm{cm}^2$ in geometry of Fig. 2. "Upstream" boundary of patterned area was inclined by 10° from normal to projected ion beam direction. Line is a guide to the eye.

The extent to which the boundary can be used to "deflect" the ripples is shown in Fig. 6. Not surprisingly, the ability of the boundary to exert a long-range influence on the alignment of ripples decays as the boundary inclination from the natural ripple orientation increases. This effect appears to limit our ability to create patterns covering arbitrary areas by controlling only the boundaries.

Although three variables (dose, beam incidence angle, pattern boundary angle) were systematically varied, we did not attempt an optimization involving other variables or combinations of these three. It is possible that conditions might be found that increase the extent to which boundaries can influence the self-organization still farther.

Linear[9] and nonlinear[10] partial differential equations (PDEs) have been proposed as descriptions of the sputter-rippling phenomenon. It is not clear whether any PDE proposed to date can describe adequately the large-aspect-ratio morphologies observed in germanium, as well as the observation that under some conditions[4] some parts of the sputtered surface actually rise above the original surface height.

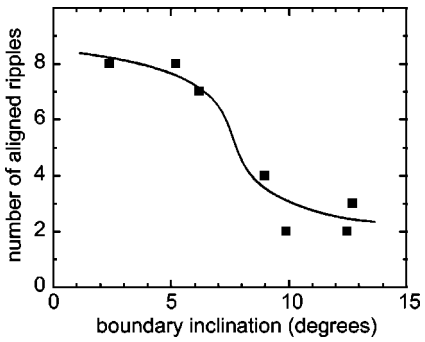

FIG. 6. Number of aligned ripples vs upstream boundary inclination angle from normal to projected ion beam direction. Milled crater was a parallelogram with two boundaries parallel to the projected ion beam direction and two boundaries inclined by the stated amount from normal to the projected ion beam direction. FIB incidence angle was 62° from surface normal and dose was $1.6 \times 10^{18}/\mathrm{cm}^2$. Line is a guide to the eye.

It is anticipated that the morphological evolution reported here will help determine the nature of the most important terms in a governing PDE.

More generally, there remains open the question of which physical effects, or which terms in a PDE, should be important in order to permit one to maximize the degree of morphology control one can exercise in the interior of a uniformly-processed area by manipulating only the boundaries of the processed area. The answer may be crucial for the future role of lithographic patterning on the smallest practical length scale to control the self-organization at yet smaller length scales in the mass production of nanoscale devices. Experiments such as this one begin to address this issue for CMOS-compatible processes.

This work was supported by the DOE through Grant No. DE-FG02-01ER45947 and by the Harvard College Research Program. We are grateful to Warren MoberlyChan for technical assistance and helpful discussions, and to H. Bola George, Alexandre Cuenat, and Wei Zhou for helpful discussions.

[1]E. Chason and M. J. Aziz, Scr. Mater. **49**, 953 (2003).

[2]S. Habenicht, K. P. Lieb, J. Koch, and A. D. Wieck, Phys. Rev. B **65**, 115327 (2002); D. P. Adams, M. J. Vasile, T. M. Mayer, and V. C. Hodges, J. Vac. Sci. Technol. B **21**, 2334 (2003).

[3]A. Cuenat and M. J. Aziz, Mater. Res. Soc. Symp. Proc. **696**, N2.8.1 (2002).

[4]W. Zhou, A. Cuenat, and M. J. Aziz, in *Microscopy of Semiconducting Materials 2003: Proceedings of the 13th International Conference on Microscopy of Semiconducting Materials*, edited by A. G. Cullis and P. A. Midgley (IOP, New York, 2003).

[5]E.-H. Cirlin, J. J. Vajo, R. E. Doty, and T. C. Hasenberg, J. Vac. Sci. Technol. A **9**, 1395 (1991).

[6]J. Erlebacher, M. Aziz, E. Chason, M. Sinclair, and J. Floro, Phys. Rev. Lett. **82**, 2330 (1999); S. Habenicht, Phys. Rev. B **63**, 125419 (2001); C. C. Umbach, R. L. Headrick, and K. C. Chang, Phys. Rev. Lett. **87**, 246104 (2001); D. Flamm, F. Frost, and D. Hirsch, Appl. Surf. Sci. **179**, 95 (2001).

[7]S. Facsko, T. Dekorsy, C. Koerdt, C. Trappe, H. Kurz, A. Vogt, and H. L. Hartnagel, Science **285**, 1551 (1999); S. Facsko, T. Dekorsy, C. Trappe, and H. Kurz, Microelectron. Eng. **53**, 245 (2000); F. Frost, A. Schindler, and F. Bigl, Phys. Rev. Lett. **85**, 4116 (2000).

[8]J. P. Biersack and L. G. Haggmark, Nucl. Instrum. Methods **174**, 257 (1980).

[9]R. M. Bradley and J. M. Harper, J. Vac. Sci. Technol. A **6**, 2390 (1988).

[10]M. A. Makeev, R. Cuerno, and A.-L. Barabasi, Nucl. Instrum. Methods Phys. Res. B **197**, 185 (2002); U. Valbusa, C. Boragno, and F. Buatier de Mongeot, J. Phys.: Condens. Matter **14**, 8153 (2002); M. Castro, R. Cuerno, L. Vazquez, and R. Gago, Phys. Rev. Lett. **94**, 016102 (2005).